

Application of LC-NMR for Characterization of Rat Urinary Metabolites of Zonampanel Monohydrate (YM872)

Kin-ya SOHDA,^{*,a} Tsuyoshi MINEMATSU,^a Tadashi HASHIMOTO,^a Ken-ichi SUZUMURA,^b Masashi FUNATSU,^b Katsuhiko SUZUKI,^a Harumitsu IMAI,^a Takashi USUI,^a and Hidetaka KAMIMURA^a

^aDrug Metabolism Laboratories, Drug Development Division, Yamanouchi Pharmaceutical Co., Ltd.; 1-1-8 Azusawa, Itabashi-ku, Tokyo 174-8511, Japan; and ^bAnalysis Research, Analysis & Metabolism Laboratories, Institute for Drug Discovery Research, Yamanouchi Pharmaceutical Co., Ltd.; 21 Miyukigaoka, Tsukuba, Ibaraki 305-8585, Japan.

Received July 5, 2004; accepted August 21, 2004

Zonampanel monohydrate (YM872) has a potent and selective antagonistic effect on the glutamate receptor subtype, α -amino-3-hydroxy-5-methylisoxazole-4-propionic acid (AMPA) receptor. Metabolic fingerprinting in rat urine after a single intravenous administration of ¹⁴C-labeled YM872 (¹⁴C-YM872) revealed the presence of two metabolites, R1 and R2. The two metabolites were semi-purified by preparative HPLC from rat urine after a single intravenous administration of non-labeled YM872, and their structures were elucidated by various instrumental analyses involving LC-NMR. The results showed that R1 and R2 have a hydroxyamino group and an amino group at the C-7 position of the quinoxalinedione skeleton, respectively. Therefore, the proposed metabolic pathway of YM872 in rats involves the reduction of the nitro group to a hydroxyamino group and then subsequent reduction to an amino group.

Key words LC-NMR; YM872; zonampanel monohydrate; urinary metabolite; α -amino-3-hydroxy-5-methylisoxazole-4-propionic acid (AMPA) receptor antagonist

Zonampanel monohydrate (YM872, Fig. 1) was discovered to be a novel competitive α -amino-3-hydroxy-5-methylisoxazole-4-propionic acid (AMPA) receptor antagonist, which is a highly water-soluble agent with the selectivity and potency for AMPA receptors.¹⁾ YM872 has been shown to provide neuroprotection in a variety of animal models of ischemia.²⁻⁴⁾

In this study, ¹⁴C-labeled YM872 (¹⁴C-YM872) was intravenously administered to rats in order to measure urinary excretion of radioactivity and metabolic fingerprinting in urine. Furthermore, two metabolites were semi-purified by preparative HPLC from rat urine after a single intravenous administration of non-labeled YM872, and their structures were elucidated by various instrumental analyses using high-resolution matrix-assisted laser desorption/ionization time-of-flight mass spectrometry (HR-MALDI-TOFMS), LC-MS, LC-MS/MS, and LC-NMR.

LC-NMR has been recently used for metabolite structure determination.⁵⁻⁷⁾ LC-NMR elucidates the structure of trace components in mixtures and unstable compounds which are easily decomposed during purification and evaporation to dryness. LC-NMR is more suitable for the two YM872 metabolites than conventional NMR because they are trace components in urine and one of them is likely to be unstable at room temperature. For these reasons, LC-NMR was selected as the method of choice.

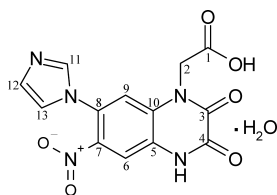


Fig. 1. Chemical Structure of Zonampanel Monohydrate ([2,3-Dioxo-7-(1*H*-imidazol-1-yl)-6-nitro-1,2,3,4-tetrahydro-1-quinoxaliny]acetic Acid Monohydrate; YM872)

Results and Discussion

Urinary excretion of total radioactivity was $75.6 \pm 7.4\%$ of dose [mean \pm standard deviation (SD) of 4 rats] from 0 to 8 h after a single intravenous administration of ¹⁴C-YM872. On the HPLC radiochromatogram of the rat urine collected from 0 to 8 h after administration, a major peak corresponding to the parent compound was observed at about 26 min and small metabolite peaks were observed at about 17 and 19.5 min (Fig. 2). Urinary excretion of radioactivity for each peak at about 17 (R1), 19.5 (R2), and 26 min (the parent compound) were $0.7 \pm 0.2\%$, $0.8 \pm 0.5\%$, and $71.5 \pm 6.3\%$ of dose (mean \pm SD of 4 rats), respectively. In the fingerprinting study, storage temperature was shown to influence urinary metabolites (data not shown). HPLC radiochromatogram of the rat urine after storage for about 24 h at room temperature showed that the peak of R1 decreased, whereas the peak of R2 increased. In contrast, there was no change after storage for about 24 h at 4 °C. The observation suggests that R1 is likely to be unstable at room temperature.

The HPLC-UV chromatogram of the rat urine collected from 0 to 6 h after administration of non-labeled YM872 also showed a major peak corresponding to the parent compound and small peaks corresponding to the metabolites, R1 and R2. These metabolites were semi-purified by repeated preparative HPLC as described in the experimental section, followed by the elucidation of their structures.

Based on LC-MS analysis, the parent compound had a protonated molecule at m/z 332. MS/MS analysis of the protonated molecule revealed fragment ions at m/z 286 and 242, which were derived from the loss of NO₂ and the loss of NO₂ and CO₂, respectively. The parent compound was analyzed by LC-NMR to compare with the metabolites. The ¹H-NMR stopped-flow spectrum of the parent compound revealed five singlet peaks. These signals were assigned as shown in Fig. 3a based on the conventional ¹H-NMR signal assignments for YM872. The peak height of H-9 is obviously larger than that of other aromatic protons. The methylene signal at H-2

* To whom correspondence should be addressed. e-mail: souda@yamanouchi.co.jp

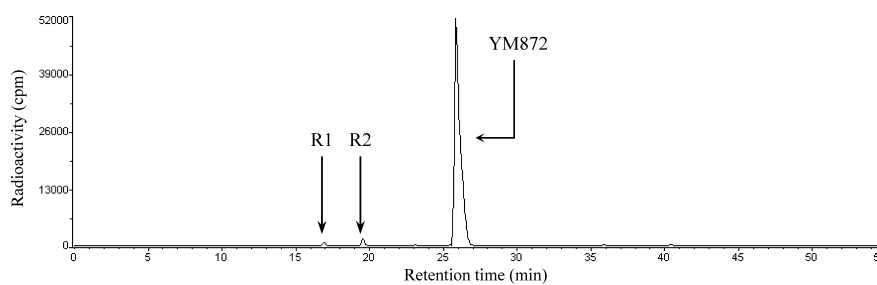


Fig. 2. HPLC Radiochromatogram of Rat Urine Collected from 0 to 8 h after a Single Intravenous Administration of ^{14}C -YM872. The metabolites R1 and R2 were designated according to their relative HPLC retention times.

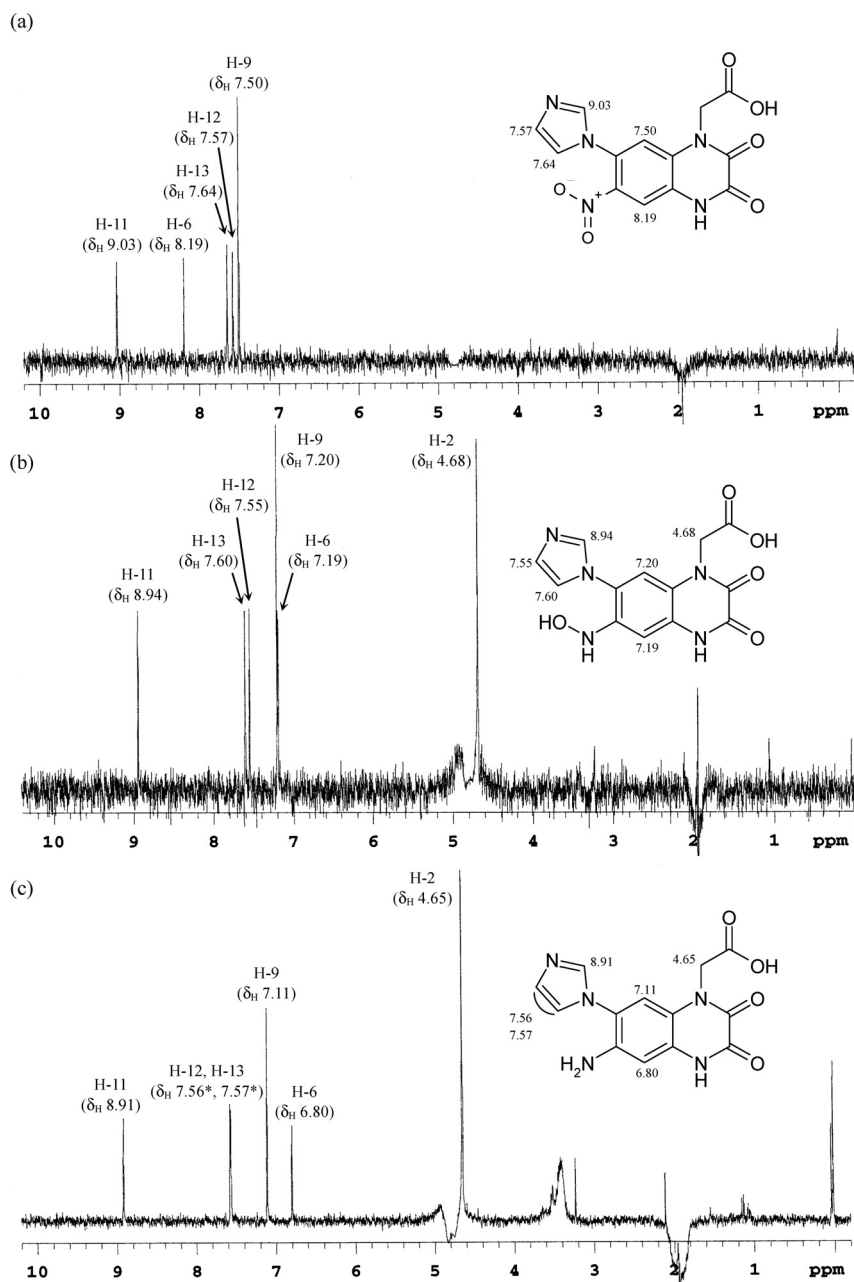


Fig. 3. ^1H -NMR Stopped-Flow Spectra of YM872 (a), R1 (b), and R2 (c)

* Exchangeable.

was not observed in the $^1\text{H-NMR}$ stopped-flow spectrum since the signal was probably suppressed by LC-NMR solvent suppression because of the overlap with the residual HOD.

The protonated molecule of R1 was observed at m/z 318, 14 Da less than that of the parent compound. MS/MS analysis of the protonated molecule revealed prominent fragment ions at m/z 301 and 300, which were derived from the loss of OH and the loss of H_2O , respectively. In addition, minor fragment ions were observed at m/z 274 and 256, which were attributed to the loss of CO_2 and the loss of CO_2 and H_2O , respectively, suggesting that the carboxyl group remained intact and a hydroxyl group existed in the molecule. The molecular formula of R1 was established as $\text{C}_{13}\text{H}_{11}\text{N}_5\text{O}_5$ by HR-MALDI-TOF-MS (Calcd for $[\text{C}_{13}\text{H}_{11}\text{N}_5\text{O}_5+\text{H}]^+$: 318.0839; Found: 318.0827). The $^1\text{H-NMR}$ stopped-flow spectrum of R1 revealed six singlets (Fig. 3b). The three aromatic protons at δ_{H} 8.94 (H-11), 7.55 (H-12), and 7.60 (H-13) exhibited almost the same chemical shifts as those of the parent compound, indicating that the imidazole ring remained intact. The two aromatic protons at δ_{H} 7.19 and 7.20 were assigned to H-6 and H-9, respectively, based on the difference in peak heights. The proton signals at H-6 and H-9 shifted upfield more than those of the parent compound, suggesting the attachment of an electron donating group at the C-7 position of the quinoxalinedione skeleton. The remaining proton signal at δ_{H} 4.68 was assigned to the methylene proton at H-2 based on the chemical shift and the integration ratio. These results showed that R1 has a hydroxyamino group at the C-7 position (Fig. 3b).

The protonated molecule of R2 appeared at m/z 302, 30 Da less than that of the parent compound and 16 Da less than that of R1, presumably due to the loss of an oxygen atom. MS/MS analysis of the protonated molecule revealed a predominant fragment ion at m/z 258, which resulted from the loss of CO_2 . In addition, a minor fragment ion was observed at m/z 241, which was ascribed to the loss of CO_2 and NH_3 , indicating that the carboxyl group remained intact and an amino group existed in the molecule. The molecular formula of R2 was established as $\text{C}_{13}\text{H}_{11}\text{N}_5\text{O}_4$ by HR-MALDI-TOF-MS (Calcd for $[\text{C}_{13}\text{H}_{11}\text{N}_5\text{O}_4+\text{H}]^+$: 302.0889; Found: 302.0893). The $^1\text{H-NMR}$ stopped-flow spectrum of R2 revealed six singlets (Fig. 3c). The three aromatic protons at δ_{H} 8.91 (H-11), 7.56* (H-12), and 7.57* (H-13) (*exchangeable) exhibited almost the same chemical shifts as those of the parent compound, suggesting that the imidazole ring remained intact. The two aromatic protons at δ_{H} 6.80 and 7.11 were assigned to H-6 and H-9, respectively, based on the difference in peak heights. The chemical shift of H-6 and H-9 decreased by 1.39 and 0.39 ppm, respectively, compared with the parent compound. These proton signals shifted upfield more than those of R1, indicating the attachment of a stronger electron donating group at the C-7 position than the

hydroxyamino group. The remaining proton signal at δ 4.65 was assigned to the methylene proton at H-2 based on the chemical shift and the integration ratio. These results showed that R2 has an amino group at the C-7 position (Fig. 3c).

The deduced structures of R1 and R2 suggest that they are formed by reduction of YM872's nitro group. The nitroreduction of aromatic nitro compounds is widely known metabolic reaction. Previous studies have demonstrated that NADPH-cytochrome *c* reductase,^{8–11} cytochrome P450,^{11,12} DT-diaphorase,^{13,14} aldehyde oxidase,^{15,16} and xanthine oxidase^{10,17–21} possess nitroreductase ability. Sugimura *et al.* have shown that rat liver can reduce 4-nitroquinoline-1-oxide to the corresponding hydroxylamine and subsequently to the corresponding amine.^{14,22} Bueding *et al.* have demonstrated that animal tissues can reduce 2,4,6-trinitrotoluene (TNT) to 4-hydroxyamino-2,6-dinitrotoluene and further reduce it to 4-amino-2,6-dinitrotoluene.¹⁷ Kato *et al.* have shown that rat liver can reduce *p*-nitrobenzoic acid to *p*-hydroxyaminobenzoic acid and subsequently to *p*-aminobenzoic acid.²³ Tatum *et al.* have demonstrated that rabbit liver can reduce 2-nitrofluorene, 4-nitrobiphenyl, and 1-nitronaphthalene to the corresponding hydroxylamines and further to the corresponding amines.¹⁶

In summary, we have shown that LC-NMR is a suitable technique for structural elucidation of YM872 metabolites, R1 and R2, found in rat urine. We were able to propose the structures of these trace components in urine by the use of LC-NMR. The results showed that R1 and R2 have a hydroxyamino group and an amino group at the C-7 position of the quinoxalinedione skeleton, respectively. Therefore, we conclude that the proposed metabolic pathway of YM872 in rats involves the reduction of the nitro group to a hydroxyamino group and then subsequent to an amino group (Chart 1).

Experimental

Preparation of Dosing Solvent Meglumine (Sigma Chemical Co., St. Louis, MA, U.S.A.) and mannitol (Sigma) were dissolved in distilled water for injection (Otsuka Pharmaceutical Co., Ltd., Tokyo, Japan) to prepare a dosing solvent containing 21 mg/ml of meglumine and 30 mg/ml of mannitol.

Animals Male Sprague-Dawley (SD) rats were purchased from Japan SLC, Inc. (Hamamatsu, Japan) at 6 weeks old and used in experiments at 7 weeks old, after acclimatization for at least 1 week. They were fasted overnight before administration.

Administration of ^{14}C -YM872 YM872 (Yamanouchi Pharmaceutical Co. Ltd., Tokyo, Japan) was dissolved in the dosing solvent to make a final concentration of 25 mg/ml. ^{14}C -YM872 (specific radioactivity 3.50 MBq/mg) synthesized at Amersham Biosciences Corp. (Piscataway, NJ, U.S.A.) was dissolved in this YM872 solution and the dosing solvent to make a final concentration of 25 mg/ml including 1.19 mg/ml of ^{14}C -YM872 (nominal concentration of radioactivity 4.17 MBq/ml). The dosing solution was intravenously administered in a bolus at a dose of 50 mg/2 ml/kg to 4 rats restrained in Ballman cages. Urine samples were collected on dry ice under protection from light from 0 to 8 h after the administration. The radiochemical purity of ^{14}C -YM872 in the dosing solution was 99.48% (no impurity peaks were observed at about 17 or 19.5 min in the HPLC radiochromatogram of the dosing solution).

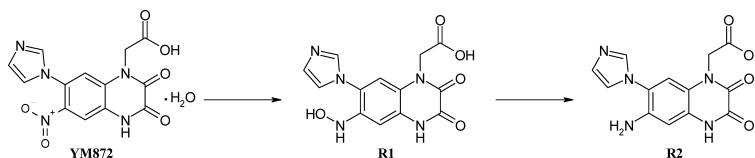


Chart 1. Proposed Metabolic Pathway of YM872 in Rats

Urinary Excretion of Total Radioactivity An aliquot (0.2 ml) of the urine sample of each rat was weighed and diluted to 10 ml with Milli-Q water purified by a Milli-Q system (Millipore Corp., Billerica, MA, U.S.A.). Then, 10 ml of Pico-Fluor 40 (PerkinElmer Life and Analytical Sciences, Inc., Boston, MA, U.S.A.) was added to an aliquot (0.2 ml) of each diluted urine sample, and the radioactivity was counted for 5 min using a liquid scintillation counter Tri-Carb 2700TR (PerkinElmer). Urinary excretion of total radioactivity in each rat was calculated using the following equation: [Urinary excretion of total radioactivity (% of dose)] = {[Concentration of radioactivity in urine (dpm/mg)] × [Amount of excreted urine (mg)] / [Administered radioactivity (dpm)]} × 100.

Metabolic Fingerprinting in Urine Immediately after the centrifugation (at 1870 × g for 15 min at 4 °C) of each urine sample, the resulting supernatant was injected into the HPLC system. The HPLC equipment and conditions were as follows: Shimadzu VP series HPLC coupled to a Radiomatic Flo-one beta radiochromatography detector (PerkinElmer); column: TSKgel ODS-80Ts (5 μm, 250 × 4.6 mm i.d., Tosoh Corp., Tokyo, Japan); guard column: TSKgel ODS-80Ts (5 μm, 15 × 3.2 mm i.d., Tosoh); mobile phase: (A) 50 mM ammonium acetate in H₂O/CH₃CN=100/1, (B) 50 mM ammonium acetate in H₂O/CH₃CN=5/1; flow rate: 1.0 ml/min; gradient condition: A/B=100/0 (0 min) → 0/100 (45 min) → 0/100 (55 min); column temperature: 35 °C. The eluent corresponding to each peak of YM872, R1, and R2 was manually fractionated every 1 min. Then, Pico-Fluor 40 (10 ml) was added to each fraction, and the radioactivity was measured in the liquid scintillation counter for 5 min. Urinary excretion of radioactivity in each peak fraction (% of dose) was calculated using the following equation: [Urinary excretion of total radioactivity in each peak fraction (% of dose)] = {[Radioactivity in each peak fraction (dpm)] / [Total radioactivity injected into HPLC (dpm)]} × {[Recovery of radioactivity through centrifugation (%)] / 100} × [Urinary excretion of total radioactivity (% of dose)]

Administration of Non-labeled YM872 YM872 was dissolved in the dosing solvent to make a final concentration of 25 mg/ml. The dosing solution was intravenously administered in a bolus at a dose of 50 mg/2 ml/kg to rats, then the rats were individually housed in metabolic cages. Urine samples were collected on dry ice under protection from light from 0 to 6 h after administration.

Purification of Urinary Metabolites The urine samples were lyophilized overnight. The resulting residue was dissolved in a small volume of HPLC mobile phase A (described below) and subsequently applied to repeated HPLC semi-purification. The HPLC equipment and conditions were as follows: Waters 2695 separation module coupled to a Waters 486 UV detector; column: TSKgel ODS-80Ts (5 μm, 250 × 4.6 mm i.d.); mobile phase: (A) 50 mM ammonium acetate in H₂O/CH₃CN=100/1, (B) 50 mM ammonium acetate in H₂O/CH₃CN=5/1, (C) 100 mM ammonium acetate in H₂O/CH₃CN=1/1; flow rate: 1.0 ml/min; gradient condition: A/B/C=100/0/0 (0 min) → 60/40/0 (18 min) → 0/0/100 (18.1 min) → 0/0/100 (30 min); column temperature: 35 °C. UV absorbance was detected at 333 nm. The eluent corresponding to each peak of R1 and R2 was manually fractionated, and each fraction was lyophilized for HR-MARDI-TOF-MS, LC-MS, LC-MS/MS, and LC-NMR analyses.

HR-MALDI-TOF-MS HR-MALDI-TOF-MS spectra were recorded on a Voyager ELITE XL mass spectrometer (Applied Biosystems, Foster, CA, U.S.A.). α -Cyano-4-hydroxycinnamic acid (CHCA) was used as a matrix and an internal standard.

LC-MS and LC-MS/MS Spectrometry MS and MS/MS spectra were recorded on a TSQ7000 mass spectrometer (Thermo Electron Corp., Waltham, MA, U.S.A.) coupled to an Agilent 1100 series HPLC. The HPLC conditions were as follows: column: Develosil C30-UG-5 (5 μm, 250 × 4.6 mm i.d., Nomura Chemical Co., Ltd., Aichi, Japan); mobile phase: H₂O/CH₃CN/formic acid=100/2/0.05; flow rate: 1.0 ml/min; column temperature: 40 °C; sheath liquid: 0.1% NH₄ in H₂O/CH₃OH=1/1 (flow rate: 0.1 ml/min). UV absorbance was detected at 333 nm. MS and MS/MS spectra were recorded in positive electrospray ionization (ESI) mode.

LC-NMR Spectrometry The HPLC equipment and conditions for LC-NMR were as follows: a ProStar 230 solvent delivery module (Varian, Inc., Palo Alto, CA, U.S.A.); column: Develosil C30-UG-5 (5 μm, 250 × 4.6 mm i.d., Nomura Chemical Co., Ltd.); mobile phase: 10 mM phosphate buffer so-

lution (pH 3) in D₂O/CD₃CN=99/1; flow rate: 1.0 ml/min; column temperature: 40 °C. UV absorption was detected at 333 nm. The Varian HPLC software was equipped with the capability for programmable stopped-flow experiments based on UV peak detection. A Unity Inova 600 spectrometer (Varian, Inc.) was operated at 599.91 MHz. For on-line LC NMR experiments, it was equipped with a ¹H {¹³C/¹⁵N} inverse detection pulsed field gradient (PFG) microflow probe (flow cell 60 μl). Probe temperature was held at 10 °C. Shimming was performed on the lock signal (D₂O). Suppression of residual CH₃CN and HOD signals was accomplished using a train of selective WET pulses with PFG. ¹H-NMR spectra were acquired in stopped-flow mode using UV absorption at 333 nm to trigger peak detection. After peak detection, the HPLC pump is stopped, trapping the peak of interest in the microflow probe. ¹H-NMR stopped-flow spectra were acquired using an acquisition time of 2.0 s, 32768 complex data points, and a spectral width of 12001.2 Hz. The ¹H-NMR stopped-flow spectra of YM872, R1, and R2 were obtained by acquiring for about 6 min (176 scans), 20 min (592 scans), and 13 h (23384 scans), respectively.

References

- 1) Kohara A., Okada M., Ohno K., Sakamoto S., Shishikura J., Inami H., Shimizu-Sasamata M., Yamaguchi T., *Soc. Neurosci. Abstr.*, **22**, 1528 (1996).
- 2) Kawasaki-Yatsugi S., Yatsugi S., Takahashi M., Toya T., Ichiki C., Shimizu-Sasamata M., Yamaguchi T., Minematsu K., *Brain Res.*, **793**, 39–46 (1998).
- 3) Kawasaki-Yatsugi S., Ichiki C., Yatsugi S., Takahashi M., Shimizu-Sasamata M., Yamaguchi T., Minematsu K., *Neuropharmacology*, **39**, 211–217 (2000).
- 4) Takahashi M., Ni J. W., Kawasaki-Yatsugi S., Toya T., Yatsugi S., Shimizu-Sasamata M., Koshiya K., Shishikura J., Sakamoto S., Yamaguchi T., *J. Pharmacol. Exp. Ther.*, **284**, 467–473 (1998).
- 5) Lindon J. C., Nicholson J. K., Sidelmann U. G., Wilson I. D., *Drug Metab. Rev.*, **29**, 705–746 (1997).
- 6) Perkins E. J., Cramer J. W., Farid N. A., Gadberrry M. G., Jackson D. A., Mattiuz E. L., O'bannon D. D., Weiss H. J., Wheeler W. J., Wood P. G., Cassidy K. C., *Drug Metab. Dispos.*, **31**, 1382–1390 (2003).
- 7) Elipse M. V. S., Huskey S.-E. W., Zhu B., *J. Pharm. Biomed. Anal.*, **30**, 1431–1440 (2003).
- 8) Kamm J. J., Gillette J. R., *Life Sci.*, **4**, 254–260 (1963).
- 9) Feller D. R., Morita M., Gillette J. R., *Biochem. Pharmacol.*, **20**, 203–215 (1971).
- 10) Wang C. Y., Behrens B. C., Ichikawa M., Bryan G. T., *Biochem. Pharmacol.*, **23**, 3395–3404 (1974).
- 11) Harada N., Omura T., *J. Biochem.*, **87**, 1539–1554 (1980).
- 12) Gillette J. R., Kamm J. J., Sasame H. A., *Mol. Pharmacol.*, **4**, 541–548 (1968).
- 13) Kato R., Takahashi A., Oshima T., *Biochem. Pharmacol.*, **19**, 45–55 (1970).
- 14) Sugimura T., Okabe K., Nagao M., *Cancer Res.*, **26**, 1717–1721 (1966).
- 15) Wolport M. K., Althaus J. R., Johns D. G., *J. Pharmacol. Exp. Ther.*, **185**, 202–213 (1973).
- 16) Tatsumi K., Kitamura S., Narai N., *Cancer Res.*, **46**, 1089–1093 (1986).
- 17) Bueding E., Jolliffe N., *J. Pharmacol. Exp. Ther.*, **88**, 300–312 (1946).
- 18) Taylor J. D., Paul H. E., Paul M. F., *J. Biol. Chem.*, **191**, 223–231 (1951).
- 19) Morita M., Feller D. R., Gillette J. R., *Biochem. Pharmacol.*, **20**, 217–226 (1971).
- 20) Tatsumi K., Kitamura S., Yoshimura H., *Chem. Pharm. Bull.*, **21**, 622–628 (1973).
- 21) Tatsumi K., Yamaguchi T., Yoshimura H., *Arch. Biochem. Biophys.*, **175**, 131–137 (1976).
- 22) Sugimura T., Okabe K., Endo H., *Gann*, **56**, 489–501 (1965).
- 23) Kato R., Oshima T., Takanaka A., *Mol. Pharmacol.*, **5**, 487–498 (1969).